NASA TECHNICAL NOTE

NASA TN D-1908

NASA TN D-1908

FLIGHT SHOCK AND VIBRATION DATA OF THE ECHO A-12 APPLICATION VERTICAL TESTS (AVT-1 AND AVT-2)

by W. B. Tereniak
Goddard Space Flight Center
Greenbelt, Maryland
and
S. A. Clevenson
Langley Research Center
Langley Station, Hampton, Va.

NATIONAL AERONAUTICS AND SPACE ADMINISTRATION • WASHINGTON, D. C. • OCTOBER 1963

TECHNICAL NOTE D-1908

FLIGHT SHOCK AND VIBRATION DATA OF THE ECHO A-12 APPLICATION VERTICAL TESTS (AVT-1 AND AVT-2)

By W. B. Tereniak

Goddard Space Flight Center

and

S. A. Clevenson

Langley Research Center

NATIONAL AERONAUTICS AND SPACE ADMINISTRATION

FLIGHT SHOCK AND VIBRATION DATA OF THE ECHO A-12 APPLICATION VERTICAL TESTS (AVT-1 AND AVT-2)

by
W. B. Tereniak
Goddard Space Flight Center
and
S. A. Clevenson
Langley Research Center

SUMMARY

This paper presents shock and vibration data measured at the base of the spacecraft adapter during the flights of Echo A-12 Application Vertical Tests numbers 1 and 2 (AVT-1 and AVT-2). A modified Thor missile was employed as the launch vehicle for each flight. Also included are data obtained from a vibration survey performed on the AVT-2 spacecraft equipment compartment prior to flight. The two sets of flight data, the vibration flight acceptance test specification, and the results of the vibration survey are compared.

It was found that levels and frequencies measured during the two flights were comparable and that the frequencies measured during flight were similar to those measured during the vibration survey. The previously written vibration flight acceptance test specification was determined to be adequate and not overly severe.

CONTENTS

FLIGHT SHOCK AND VIBRATION DATA OF THE ECHO A-12 APPLICATION VERTICAL TESTS (AVT-1 AND AVT-2)

(Manuscript Received May 1, 1963)

by
W. B. Tereniak
Goddard Space Flight Center
and
S. A. Clevenson
Langley Research Center

INTRODUCTION

One of the many obstacles that a spacecraft must overcome in order to operate successfully in space is the severe environment imposed during the launch and powered flight phases. To assure that the spacecraft is capable of surviving such environments, it is subjected to extensive environmental testing. In order to establish adequate environment simulation criteria, flight data must be obtained. Two of these environments, shock and vibration, were measured during the Echo A-12 Application Vertical Tests numbers 1 and 2 (AVT-1 and AVT-2). Prior to AVT-1 neither flight shock nor vibration data had been measured at the Thor interface. A limited amount of flight vibration data had been measured in the Thor forward compartment, and has been published. However, it was felt that vibration data measurements at the Thor interface, which could be used to determine Thor vibration inputs to the adjoining spacecraft or rocket motor, would be of great value in establishing environmental test criteria for spacecraft or flight hardware located above the Thor booster.

Consequently, vibration measurements were made during the flights of AVT-1 and AVT-2 with three vibration accelerometers at the base of the spacecraft adapter, oriented to measure vibrations in three mutually perpendicular axes: (1) along the longitudinal axis, (2) along the pitch axis, and (3) along the yaw axis.

Both flights were launched from Cape Canaveral, Florida, the AVT-1 on January 15, 1962, and the AVT-2 on July 17, 1962. The *primary* objective of these tests was to study and observe the deployment and inflation characteristics of the 135-foot space inflatable rigidized sphere and to determine its stability for orbital launch. One of the *secondary* objectives was to measure the shock and vibration environment to which the spacecraft would be subjected during these tests.

The purpose of this paper is to present the flight shock and vibration data measured during the flights of AVT-1 and AVT-2 and to indicate the adequacy of the previously determined shock and vibration environmental test specifications. The flight data will be compared (1) with the vibration

response data obtained from the ground vibration survey of the spacecraft equipment compartment of the AVT-2 launch vehicle, and (2) with the environmental test specification. These data are presented in the forms of overall accelerations as a function of flight time; relative vibratory levels as a function of frequency at various times of interest, such as liftoff, fairing separation, and spacecraft separation; power spectral density as a function of frequency; and probability density curves. In addition the vehicle is described, and typical time histories of flight performance are given.

DESCRIPTION OF SPACECRAFT AND LAUNCH VEHICLE

A photograph showing the AVT-2 vehicle on its launch pad at Cape Canaveral prior to liftoff is given in Figure 1. Figure 2 shows the spacecraft, containing the 135-foot inflatable sphere and the spacecraft mounting adapter. The general arrangement of the vehicle is given in Figure 3. The configurations of the launch vehicles were identical to the extent that their differences would not influence their dynamic characteristics. The main booster employed was the modified Douglas Aircraft Company (DAC) Model DM-21 Thor missile with its Bell Telephone Laboratory guidance system located in the Thor forward compartment.

Figure 1—AVT vehicle on launch pad at Atlantic Missile Range.

Mounted above the Thor forward compartment was the spacecraft equipment compartment, which housed the coast attitude control system; television camera system; recoverable data capsule and its separation mechanism; and electrical power, signal distribution, and sequence command systems. The spacecraft adapter was bolted to the top of the spacecraft equipment compartment. The spacecraft in turn was secured to the adapter with a marman clamp held together with explosive bolts. The spacecraft was housed in an oblate spheroid canister, and used a linear-shaped charge to separate its halves and allow inflation of the 135-foot sphere.

Inflation of the sphere in space was accomplished by utilizing a subliming powder inside the balloon. Fifty-two pounds of acetamide provided the pressure for inflating the AVT-1 sphere, while 52 pounds of benzoic acid was used for the AVT-2 sphere. Also inside the balloons was 10 pounds of red dye to be used as an easily distinguishable visual indicator of balloon rupture or leakage.

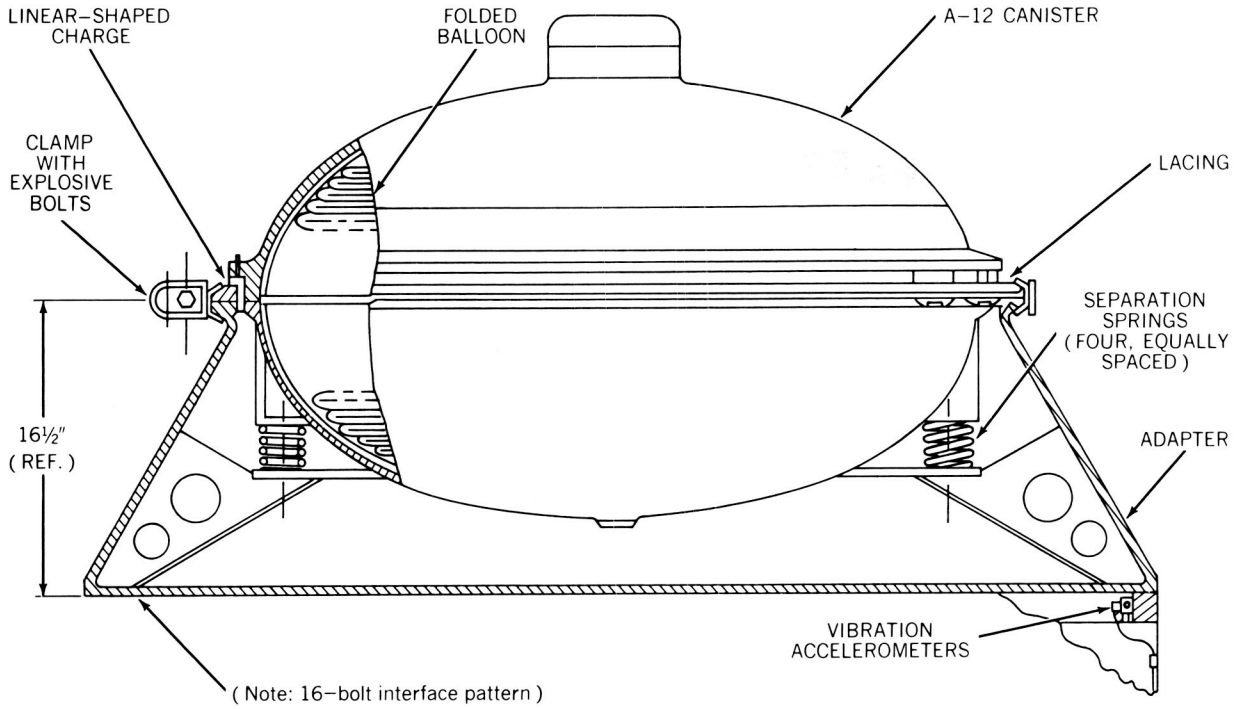

Figure 2—AVT spacecraft and adapter.

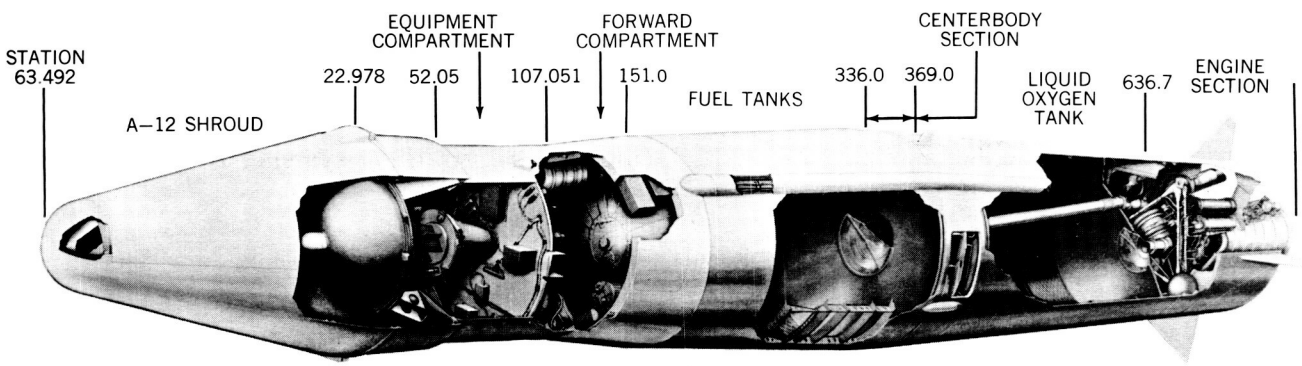

Figure 3—Cutaway view of vehicle.

INSTRUMENTATION AND DATA REDUCTION

The AVT vehicles were instrumented, at Langley Research Center's request, with three vibration transducers located at the base of the spacecraft adapter and oriented to measure vibrations in the three principal axes. The selection and installation of the three-channel measuring system, and performance of all system calibration tests, were accomplished by the Douglas Aircraft Company.

Three piezoelectric vibration accelerometers were mounted at vehicle station 52.05 on the yaw left axis at the top of the spacecraft equipment compartment, as shown in Figure 4. Accelerometer

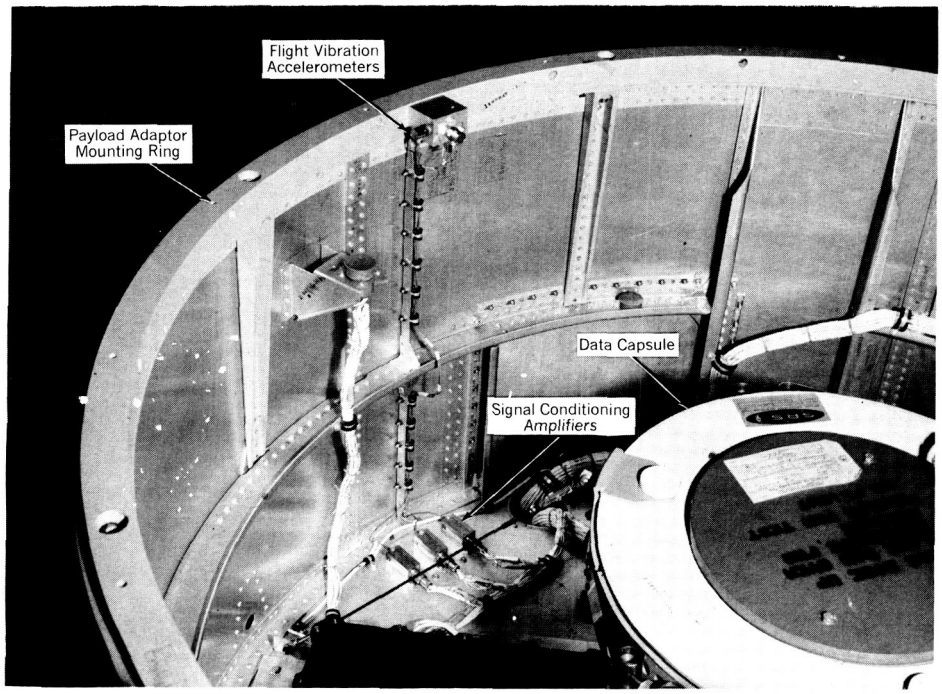

Figure 4—AVT flight accelerometer locations.

signals were conditioned by "charge" amplifiers located on the main shelf of the equipment compartment. The output of each amplifier was filtered by a low pass filter before passing into its respective voltage controlled oscillator (VCO). The vibration measuring systems for both flights are considered to be identical except for maximum signal capability. A block diagram of the flight vibration measuring system and a table summarizing the characteristics of the two flight systems are shown in Figure 5.

Figure 6 gives the frequency response curves for both flight systems. The vibration data were transmitted via the vehicle performance telemeter, located in the Thor centerbody section. This telemeter was a Pulse Duration Modulation/Frequency Modulation/Frequency Modulation (PDM/FM/FM) system, with nine continuous data subcarrier channels available. The vibration system incorporated channels 13, A, and C for the yaw, pitch, and longitudinal axis accelerometers, respectively. Composite FM data were received and recorded by both Douglas Aircraft Company and Goddard Space Flight Center (GSFC). A magnetic tape record of the composite FM data, obtained from the GSFC Telemeter 2 Ground Station, was consequently reduced.

The data were reduced, using the system given in Figure 7, by GSFC. The composite FM data were played into discriminators to restore the data to the analog form. Discriminator outputs were then filtered with low pass filters having 3 db down points of 2100 cps for subcarrier channels A and C and 1200 cps for channel 13. From this point the vibratory acceleration data were played into an oscillograph for composite level and narrow-band level versus time records, and into a root-mean-square (rms) level recorder for rms level versus time displays. Power spectral density (PSD) and

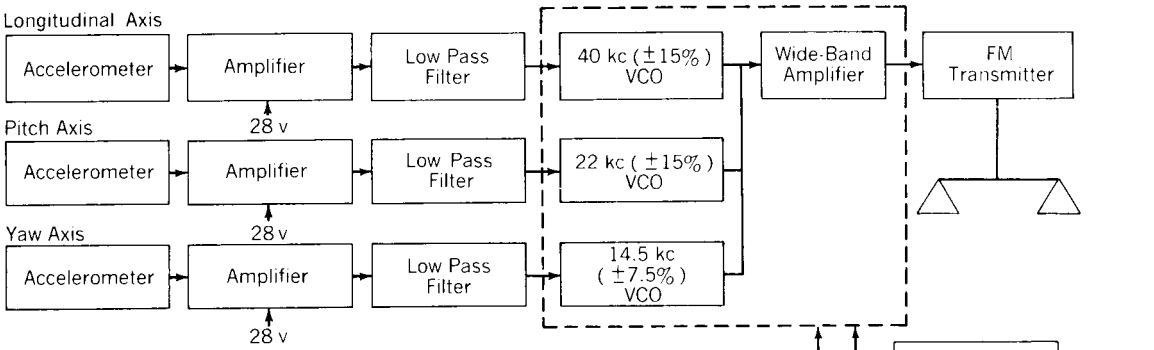

AVT Measuring System Characteristics

Axis	Subcarrier Center Freq. (kc)	Percent Deviation	Band Edge Amplitude (g-peak)
AVT-1			
Longitudinal	40	±15	± 10
Pitch	22	±15	± 15
Yaw	14.5	±7.5	± 10
AVT-2			
Longitudinal	40	±15	±15
Pitch	22	±15	±15
Yaw	14.5	±7.5	±15

Figure 5—AVT flight shock and vibration measuring system.

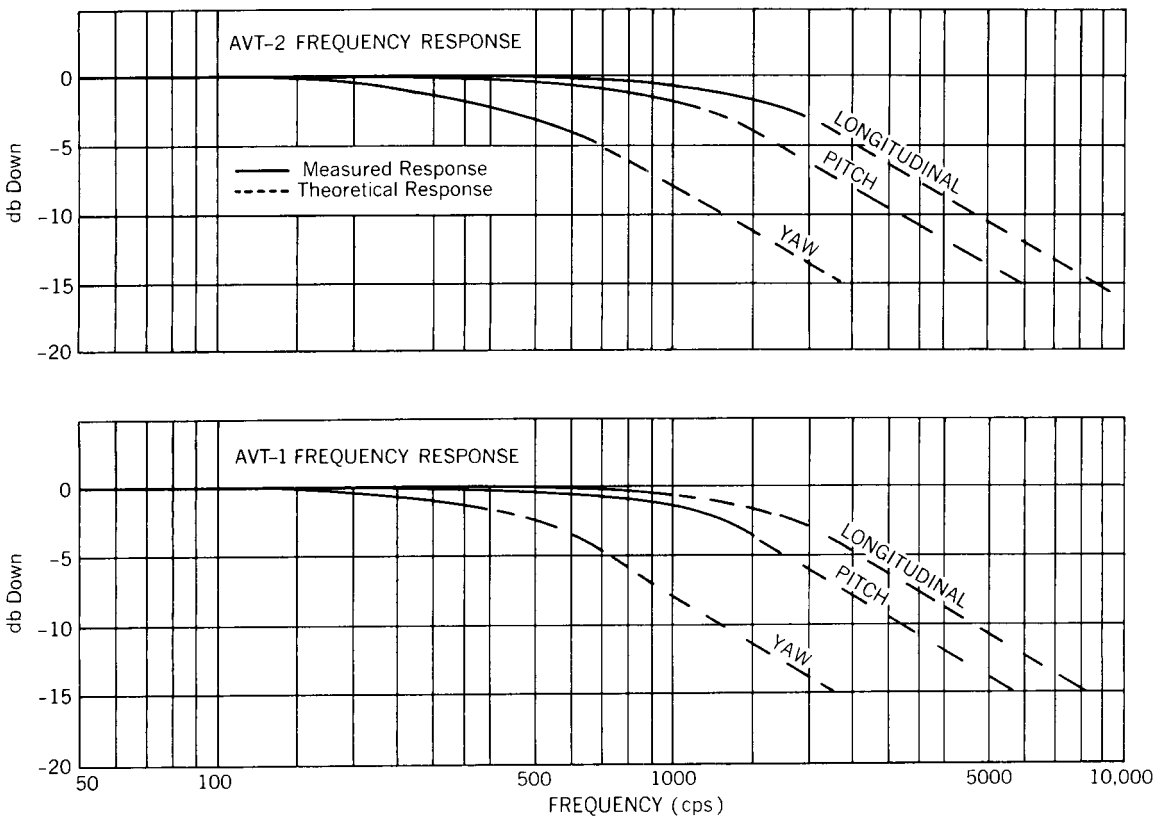

Figure 6—AVT measuring system frequency response curves.

probability density records were obtained by first re-recording a 2-second time-sample continuous tape loop of the composite FM data at the point of interest. The loop data were then discriminated and filtered, as above, and paralleled into a PSD analyzer and a probability density analyzer. The results of the PSD analysis were corrected for the frequency response of the measuring systems by multiplying the indicated level at each frequency by twice the inverse of the attenuation given in Figure 6. However, corrections for the frequency response have not been applied to the other types of analyses–that is, rms, composite, etc.

Analysis of the transient shock data during liftoff, fairing separation, and payload ejection was accomplished by making a continuous tape loop including the transient data and directing the tape output into a spectral wave analyzer. The wave analyzer plot indicated the predominate amplitudes and frequencies of the complex wave caused by the transient vibration.

FLIGHT TIME HISTORY

It is appropriate to mention the flight time history of AVT-1 and AVT-2 as a reference for the flight vibration data. Typical time histories of longitudinal steady-state acceleration, velocity, and altitude are shown in Figure 8.

Table 1 lists the sequence of events and their predicted time of occurrence. At T+144.3 seconds, main engine cutoff (MECO) occurs; and, at T+146.3 seconds, the nose fairing is ejected. At T+164.3 seconds, the payload canister is ejected with a forward velocity differential of 5.5 feet/second; and, at T+165.3 seconds, the retrorockets on the booster are ignited to cause an additional velocity differential of -8 feet/second between the booster and the payload canister. At T+185 seconds a linear-shaped charge

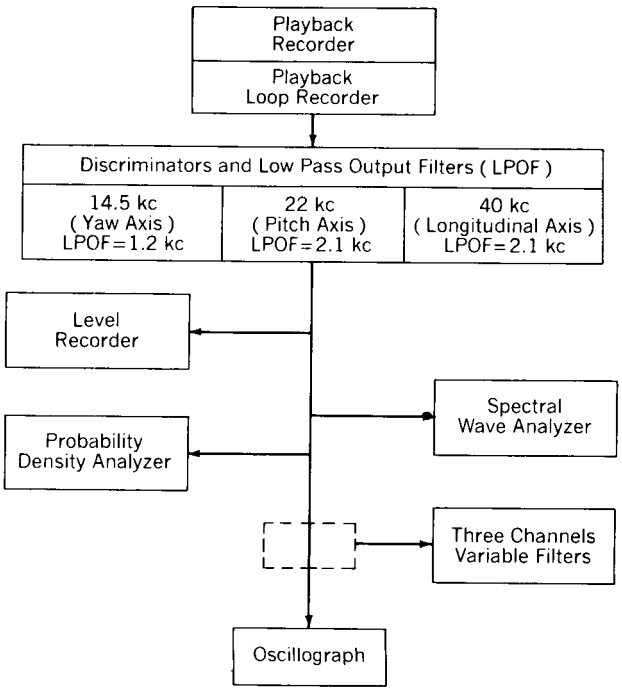

Figure 7—AVT data reduction system.

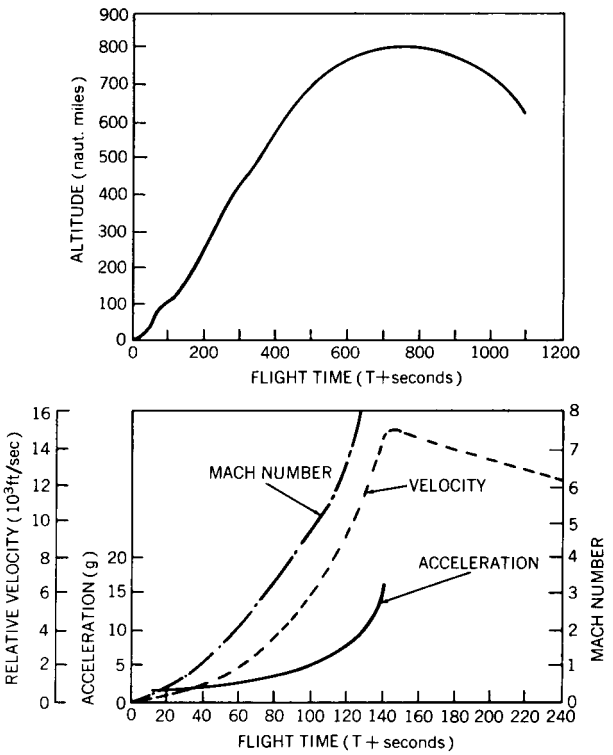

Figure 8—Typical AVT flight parameters.

is ignited to blow the halves of the payload canister apart at a relative velocity of about 50 feet/second to allow the 135-foot rigidized sphere to inflate. The inflation is observed by real-time television and is recorded on a camera that is ejected at T+1355 seconds and is later recovered.

RESULTS AND DISCUSSION

Overall Vibration Levels

Real-time oscillograph records of the composite vibratory accelerations for the longitudinal, pitch, and yaw axes measured during the flight of AVT-1 are given in Figure 9. AVT-2 real-time composite levels are given in Figure 10. Maximum levels, excluding transients, were found to occur at T+39 seconds for both flights. These relatively high levels are attributed to aerodynamic buffeting at transonic speeds and maximum dynamic pressure. The accuracy of these high longitudinal levels cannot be determined, as they are beyond the calibrated range and probably in the nonlinear range of the system. The optimum range for the AVT-2 longitudinal axis was ± 15 g-peak; however, levels of 24.7 g-peak were read, with linearity assumed above this range. These signals were not clipped, and therefore the rms analysis for AVT-2 is considered valid except for the possibility of nonlinearity (linearity not established above 16 g-peak). In the case of AVT-1 the longitudinal channel was clipped from T+35 to T+50 seconds. The optimum range for this channel was ± 10 g-peak; however, clipping occurred at approximately 18 g-peak as indicated in Figure 9.

Table 1

Typical Sequence of Events and Predicted Event Times for the AVT Vehicles.

TIME (seconds)	EVENT
T+0	(1) Start flight control programmer (2) Uncage gyros
T+2	Start roll program (-0.71086 deg/sec)
T+9	Stop roll program
T+10	Start first pitch command (-0.569 deg/sec)
T+50	Start second pitch command (-0.433 deg/sec)
T+65	Start third pitch command (-0.302 deg/sec)
T+80	First control system gain change
T+90	Second control system gain change
T+93	Start fourth pitch command (+1.4423 deg/sec)
T+134	Start fifth pitch command (-5.86 deg/sec)
T+139	Stop pitch program
T+140	Retrorocket cover ejection Enable MECO circuitry
T+144.3	MECO
T+144.3	Start sequence command programmer
T+146.3	Fairing ejection
T+149.3	F/C timer stop
T+153.3	(1) VECO (Vernier Engine Cutoff) (2) Transfer control to coast attitude system
T+159.3	Start motion picture camera
T+164.3	Separate payload
T+165.3	Ignite retrorocket
T+1344.3	Arm data capsule
T+1349.3	Cut data capsule wires
T+1355.1	Eject data capsule
T+1364.3	Motor reverse

Figure 11 indicates how closely the overall rms vibratory levels measured on AVT-2 compare with those measured on AVT-1. The levels for the accelerations measured on AVT-1 and AVT-2 are given as one curve for the pitch axis and one curve for the yaw axis, since there was less than

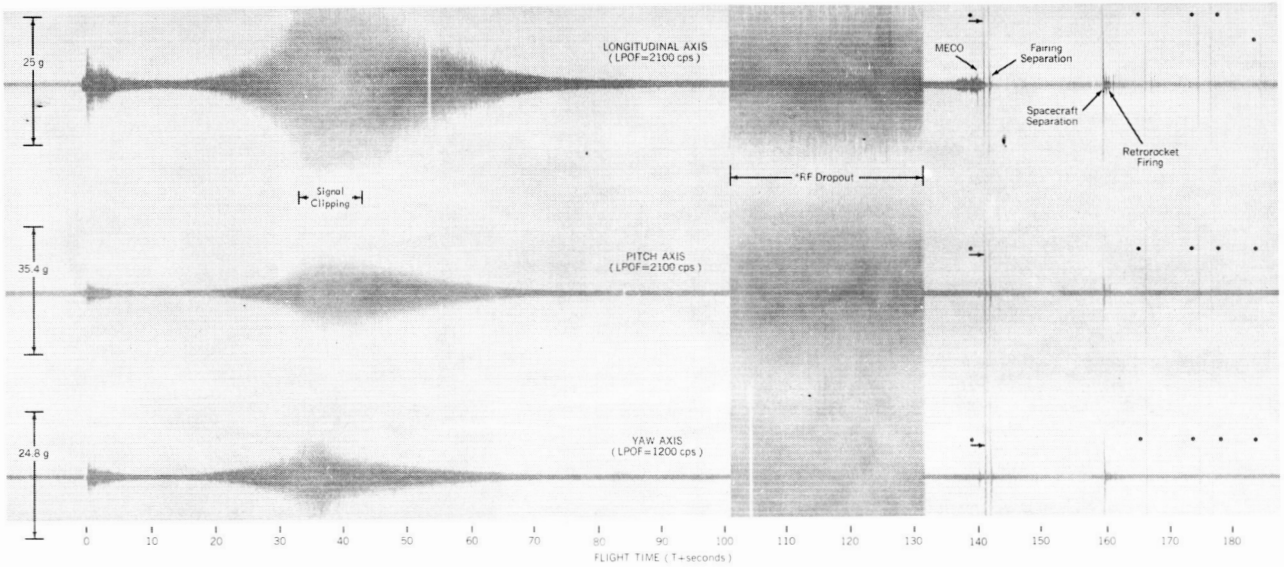

Figure 9—AVT-1 composite levels vs. flight time. (Paper speed, 0.1 in./sec)

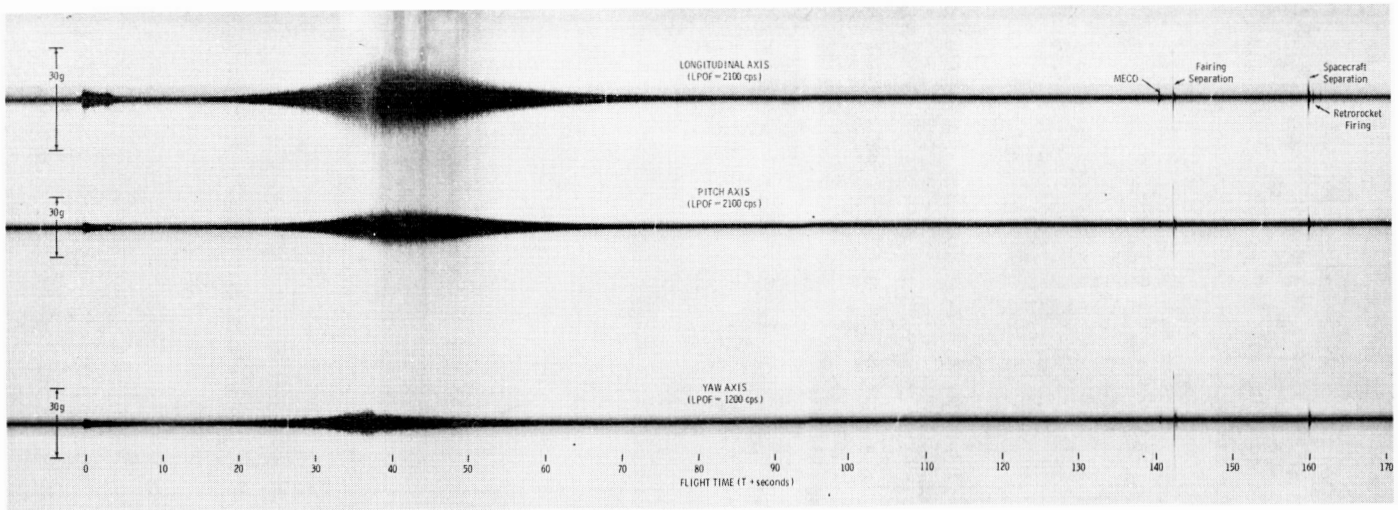

Figure 10—AVT-2 composite levels vs. flight time. (Paper speed, 0.1 in./sec)

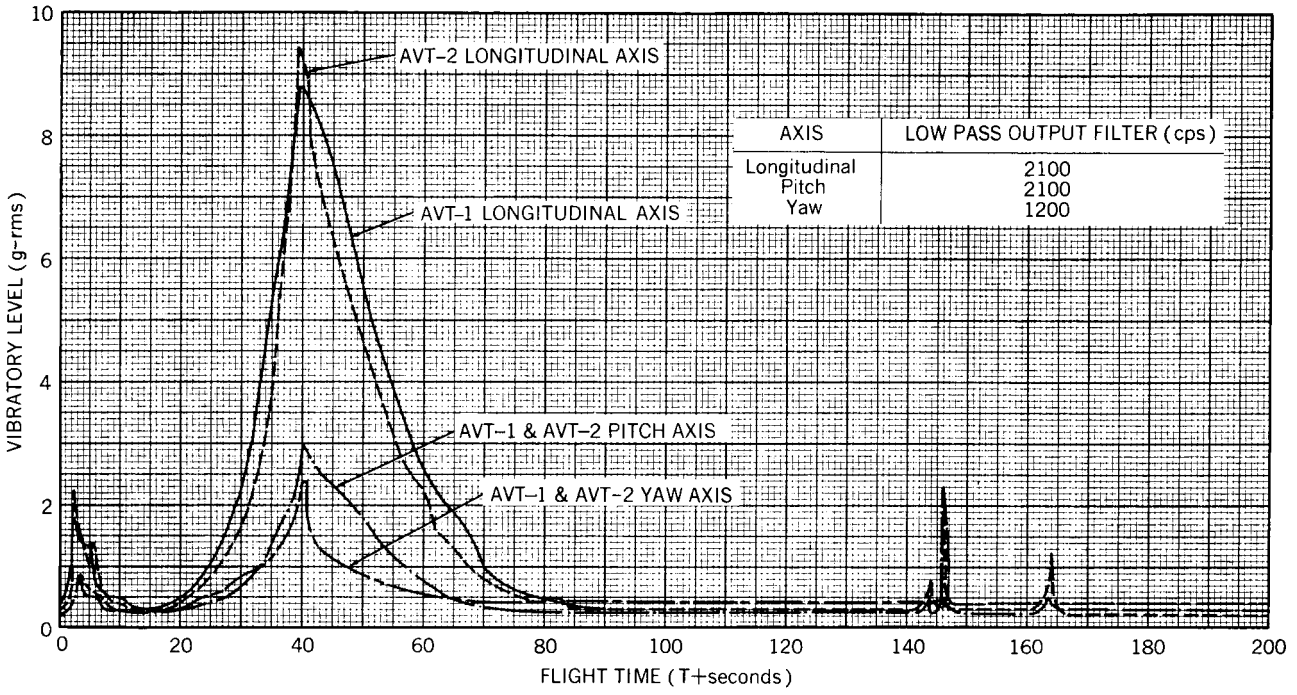

Figure 11—AVT-1 and AVT-2 rms levels vs. flight time.

10 percent difference in level between the two flights. The accelerations in the longitudinal direction closely agree except for the clipped region of AVT-1. During the AVT-1 flight there were two periods of radio frequency signal dropout where no data were received; AVT-2 experienced no such dropouts. It is significant that at AVT-2 liftoff (T+2 seconds) the value of acceleration measured on the longitudinal axis was 2.2 g-rms, whereas at approximately Mach 1 (T+39 seconds) the acceleration level was 9.4 g-rms. The measured vibration level of 9.4 g-rms is somewhat greater than that indicated by previous measurements made in the forward compartment during flights of the Thor booster. A comparison of AVT-1, AVT-2, and previous Thor flight data—at the main event times—is given in Table 2.

Differences in flight-measured vibratory levels between AVT and previous Thor flights may be accounted for by differences in transducer location, mass loading, and stiffness of the mounting structure and by differences in the thrust output of the Thor booster (AVT-1 and AVT-2 had 10 percent greater thrust than previous Thor boosters). In general, the previous low measurements were obtained from transducers located on the central bulkhead in the Thor forward compartment, whereas on AVT-1 and AVT-2 the transducers were located on the inner circumference of the structural attach ring at the top of the spacecraft equipment compartment (see Figure 3).

"Transient" Vibrations

The composite vibratory records (Figures 9 and 10) clearly indicate the vibrations excited by liftoff, MECO, fairing separation, and spacecraft separation. These vibrations are short in duration

Table 2
Comparison of AVT-1, AVT-2, and Thor Flight Data at Main Event Times
(Vibration Level, g-rms).

Event	*AVT-1			*AVT-2			Previous Thor Data		
	Longitudinal Axis	Pitch Axis	Yaw Axis	Longitudinal Axis	Pitch Axis	Yaw Axis	Longitudinal Axis	Pitch Axis	Yaw Axis
Main engine ignition	1.8	0.93	0.63	2.2	0.8	0.8	1.7	3.7	Not reported
Mach 1	8.8†	3.2	2.5	9.4	3.0	2.4	—	—	↓
Maximum dynamic pressure	3.5	1.6	0.62	4.7	1.6	0.84	1.7	3.2	
Main engine cutoff	0.35	0.45	0.1	0.95	0.47	0.54	—	0.5	

*AVT low pass output filters at 2.1, 2.1, and 1.2 kc for longitudinal, pitch, and yaw axes respectively.
†Signal clipped, and level not considered valid.

and relatively high in level. Overall levels measured during fairing separation and spacecraft separation are beyond the optimum signal range of the measuring channels. These signals are in the nonlinear range of the system and may have been "clipped" by the limiter circuit in the charge amplifier. However, it was felt that a spectral analysis of these data would be enlightening.

A tabulation of the results of the qualitative analysis performed on the vibrations excited by the above mentioned events of both flights is given in Table 3. The data were reduced by re-recording a continuous 1-second loop that included the transient vibration, and were then played back into a spectral wave analyzer that employed a 20-cps bandwidth filter. The levels presented are relative, since the time duration of the vibration signal was considerably shorter than the analyzer RC averaging time (1 second) used. The tables summarizing the predominant frequencies indicate that as a result of shocklike excitation certain resonant frequencies are excited. At liftoff these frequencies are excited by both shocklike and acoustic excitations. It is noteworthy that the frequencies are similar in value for these events. This similarity indicates that these high frequencies (greater than 200 cps) are due to a more localized response–that is, from the Thor spacecraft equipment compartment–and are not indicative of the response of the entire vehicle. The previous statement is based on the fact that the mass varies during powered flight and, in turn, varies the vibratory modes of the vehicle.

Figure 12 gives three of the low frequencies excited during AVT-2 liftoff; 17 cps is seen on the longitudinal axis, 8 cps on the pitch axis, and 11 cps on the yaw axis. Figure 13 gives the 45-cps signal, for the three principal axes, excited during liftoff of AVT-2. A tabular summary of the low frequency data obtained during liftoff and MECO of AVT-1 and AVT-2 is given in Table 4. The accuracy of the low frequency (< 50 cps) vibratory levels is questionable, since the frequency response of the measuring system below 50 cps was not measured.

Table 3

Summary of Predominant "High" Frequencies and Relative Vibratory Levels Measured on the AVT-1 and AVT-2 Principal Axes.*

Liftoff				Main Engine Cutoff				Fairing Separation				Spacecraft Separation			
AVT-1		AVT-2		AVT-1		AVT-2		AVT-1		AVT-2		AVT-1		AVT-2	
Freq. (cps)	Level	Freq. (cps)	Level	Freq. (cps)	Level	Freq. (cps)	Level	Freq. (cps)	Level	Freq. (cps)	Level	Freq. (cps)	Level	Freq. (cps)	Level
Longitudinal Axis															
130	0.05	130	0.09	170	0.02	140	0.13	–	–	–	–	–	–	–	–
–	–	–	–	230	.02	280	.04	225	0.04	230	0.15	–	–	–	–
300	.05	330	.09	330	.02	340	.04	–	–	350	.19	–	–	350	0.10
430	.08	430	.32	380	.04	400	.03	420	.04	420	.24	410	0.08	440	.12
510	.12	–	–	480	.01	500	.02	–	–	480	.30	–	–	520	.12
585	.15	580	.49	570	.01	–	–	575	.11	570	.58	580	.08	580	.11
–	–	640	.60	620	.02	–	–	–	–	650	.33	–	–	670	.48
–	–	680	.51	700	.02	–	–	–	–	–	–	710	.13	–	–
760	.10	780	.41	750	.01	–	–	770	.08	780	.43	790	.23	–	–
–	–	–	–	800	.03	800	.01	–	–	–	–	–	–	800	.36
–	–	830	.35	850	.02	–	–	–	–	850	.52	840	.25	850	.48
890	.15	–	–	920	.02	–	–	910	.05	–	–	–	–	–	–
970	.11	960	.43	990	.01	950	.01	–	–	960	.86	–	–	–	–
1070	.19	1030	.57	–	–	1040	.01	1060	.09	1020	.24	1060	.26	1010	.55
1200	.11	1160	.31	1190	.40	–	–	1170	.04	1120	.29	–	–	–	–
–	–	1260	.25	–	–	1240	.01	1270	.04	–	–	1280	.09	1220	.26
1320	.09	1340	.16	1350	.01	–	–	–	–	–	–	1310	.09	1340	.21
1420	.08	–	–	–	–	–	–	1400	.08	1450	.22	1420	.09	–	–
–	–	1490	.27	–	–	–	–	1510	.05	–	–	1500	.09	1490	.14
1580	.07	1600	.05	–	–	–	–	–	–	–	–	–	–	–	–
1710	.04	1700	.05	–	–	–	–	–	–	1700	.11	–	–	–	–
–	–	1780	.10	–	–	–	–	1800	.02	–	–	1770	.06	1800	.07
Pitch Axis															
–	–	–	–	–	–	110	0.08	–	–	–	–	133	0.12	110	0.12
–	–	–	–	180	0.05	150	.07	–	–	–	–	–	–	170	.11
200	0.06	210	0.08	–	–	210	.05	220	0.20	220	0.22	210	.11	–	–
240	.09	260	.16	–	–	280	.03	–	–	260	.28	–	–	260	.08
310	.06	340	.10	330	.04	330	.07	340	.08	–	–	–	–	310	.09
–	–	–	–	380	.03	–	–	390	.10	360	.14	–	–	–	–
460	.09	470	.12	470	.02	–	–	440	.13	440	.10	440	.07	440	.09
–	–	540	.11	–	–	500	.02	550	.08	–	–	–	–	520	.05
–	–	–	–	580	.02	–	–	–	–	600	.17	–	–	620	.09
650	.06	640	.04	–	–	–	–	–	–	650	.15	650	.08	650	.07
–	–	700	.09	–	–	680	.01	–	–	–	–	–	–	–	–
–	–	–	–	740	.03	–	–	–	–	–	–	–	–	740	.04
–	–	790	.04	–	–	800	.01	780	.10	780	.14	810	.08	820	.11
830	.05	860	.10	860	.03	–	–	–	–	–	–	–	–	–	–
900	.05	–	–	–	–	–	–	920	.09	–	–	–	–	–	–
980	.04	970	.08	960	.04	–	–	–	–	–	–	990	.07	1000	.05
1050	.04	1030	.07	1030	.04	–	–	1060	.08	1030	.01	1060	.07	–	–
1100	.03	–	–	1080	.04	1100	.01	–	–	1100	.23	–	–	1100	.10
–	–	1160	.07	1170	.09	–	–	–	–	–	–	–	–	–	–
–	–	–	–	1210	.05	–	–	–	–	–	–	–	–	1220	.06
1290	.04	1260	.07	1205	.05	–	–	1260	.07	–	–	–	–	–	–
–	–	–	–	–	–	–	–	1340	.08	1370	.19	1350	.07	1340	.06
1440	.03	–	–	–	–	1470	.02	1500	.06	–	–	1480	.05	1460	.05
1650	.03	–	–	–	–	–	–	1680	.06	1650	.12	1640	.06	1650	.06
–	–	1810	.04	–	–	1880	.02	1800	.05	1850	.06	1830	.05	1850	.04
Yaw Axis															
–	–	130	0.05	–	–	140	0.04	170	0.17	–	–	140	0.12	130	0.18
220	0.12	–	–	180	0.09	200	.03	210	.39	–	–	200	.12	–	–
260	.10	230	.13	–	–	–	–	–	–	250	0.04	250	.07	250	.18
–	–	300	.14	–	–	270	.02	280	.08	–	–	280	.07	–	–
–	–	350	.18	330	.11	330	.05	320	.09	340	.03	320	.05	340	.24
–	–	–	–	–	–	–	–	420	.14	420	.03	410	.04	430	.12
440	.09	–	–	450	.06	–	–	450	.08	460	.02	–	–	–	–
490	.07	480	.12	500	.08	–	–	–	–	530	.02	520	.04	–	–
–	–	600	.10	620	.09	600	.01	560	.05	600	.02	–	–	620	.09
650	.05	–	–	680	.09	–	–	–	–	670	.02	650	.04	670	.10
780	.05	770	.07	750	.10	–	–	770	.06	–	–	–	–	780	.06
820	.05	–	–	–	–	800	.01	–	–	800	.01	810	.03	–	–
–	–	840	.07	850	.12	–	–	830	.05	850	.02	850	.03	–	–
980	.04	–	–	950	.12	–	–	–	–	–	–	–	–	–	–
–	–	1000	.04	1000	.10	–	–	–	–	–	–	–	–	–	–
1040	.03	1080	.03	–	–	1070	.01	–	–	1030	.01	–	–	1030	.04
–	–	–	–	1120	.10	–	–	–	–	–	–	–	–	–	–
–	–	–	–	1160	.19	–	–	–	–	–	–	–	–	–	–
–	–	1270	.02	1280	.08	–	–	–	–	–	–	–	–	1280	.02
–	–	1380	.01	1390	.07	–	–	–	–	–	–	–	–	–	–
–	–	1740	.01	–	–	–	–	–	–	–	–	–	–	–	–

*All levels are relative; analysis filter bandwidth, 20 cps.

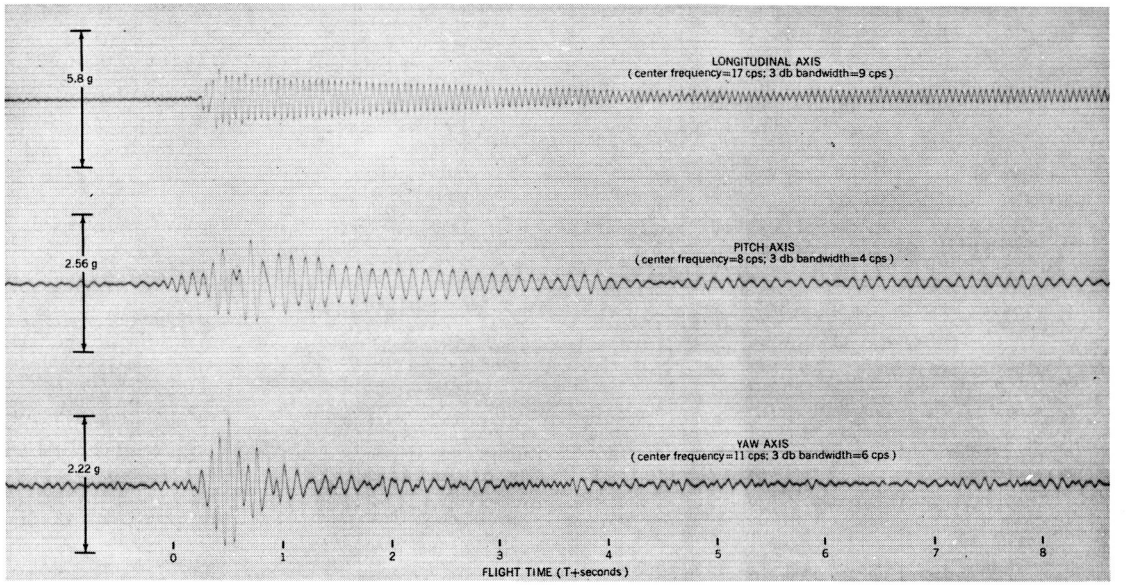

Figure 12—AVT-2 discrete frequencies measured at liftoff. (Paper speed, 1.6 in./sec)

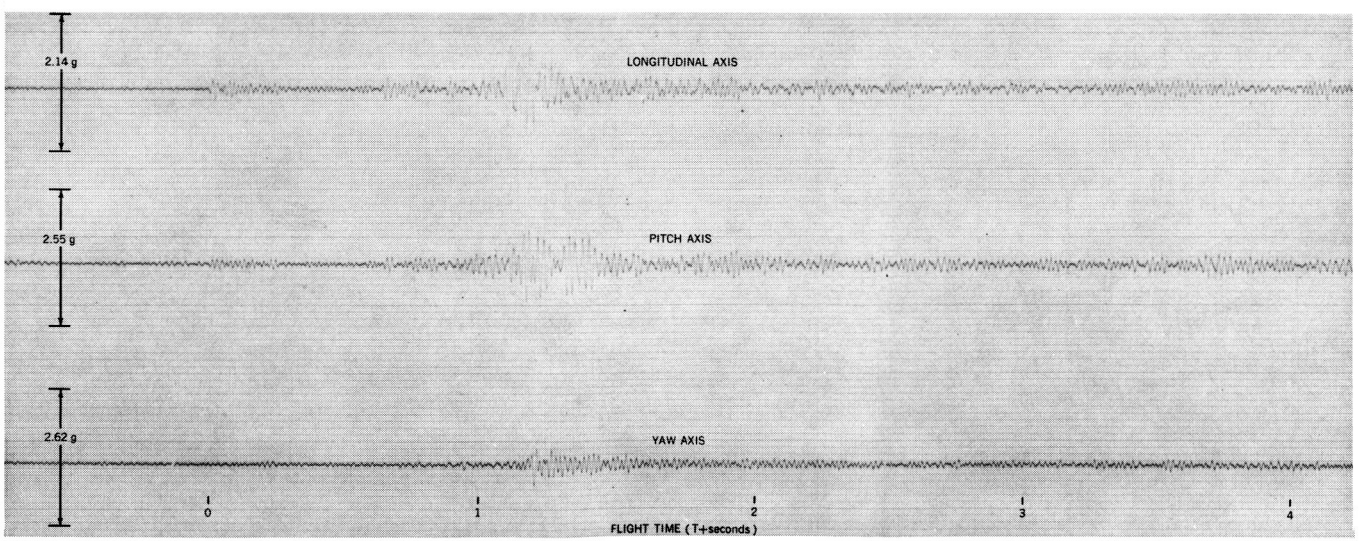

Figure 13—AVT-2 discrete frequencies measured at liftoff. (Paper speed, 4 in./sec; center frequency, 45 cps; 3 db bandwidth, 24 cps.)

Table 4

Summary of AVT Low Frequencies at Their Maximum Level.

Longitudinal Axis				Pitch Axis				Yaw Axis*			
AVT-1		AVT-2		AVT-1		AVT-2		AVT-1		AVT-2	
Freq. (cps)	Level (g-pk)	Freq. (cps)	Level (g-pk)	Freq. (cps)	Level (g-pk)	Freq. (cps)	Level (g-pk)	Freq. (cps)	Level (g-pk)	Freq. (cps)	Level (g-pk)
Liftoff											
17	1.8	17	1.0	8	0.70	8	0.5	11	1.4	11	1.1
22	2.0	–	–	–	–	9	.80	22	.70	–	–
33	1.6	–	–	–	–	11	1.0	33	.50	–	–
44	1.3	45	1.0	22	.40	–	–	–	–	45	.30
57	1.8	–	–	33	.40	–	–	57	.70	–	–
–	–	–	–	–	–	45	.90	–	–	–	–
–	–	–	–	57	.80	–	–	–	–	–	–
Main Engine Cutoff											
–	–	32	0.76	–	–	52	0.3				
–	–	42	.65	–	–	58	1.1				
55	0.4	55	.65	87	0.69	–	–				
95	.2	–	–	116	.87	–	–				
122	.91	–	–								
–	–	137	2.8								

*Yaw axis has no significant levels in the 5-150 cps range during main engine cutoff.

Random Vibrations

As shown in Figure 11, the overall rms vibratory level begins to build up again at about T+20 seconds and reaches a point of inflection at T+39 seconds, at a level of 9.4 g-rms for AVT-2. This buildup in level, which occurs in the transonic region of flight, is attributed to the random excitation caused by aerodynamic buffeting.

Power spectral density (PSD) plots are given in Figures 14 through 16 for the three axes measured during the flights of AVT-1 and AVT-2. The data sample loops for both flights were made at maximum rms level (about T+38 to T+40 seconds). AVT-1 longitudinal axis data are an exception, since signal "clipping" occurred during this time; because of clipping, the loop was obtained at T+31 to T+33 seconds. The PSD plots show that the spectra are discrete in nature with peak values at frequencies closely associated to those measured during the events of liftoff, MECO, etc. Table 5 compares the predominant frequencies of the PSD plots of the longitudinal axes of AVT-1 and AVT-2

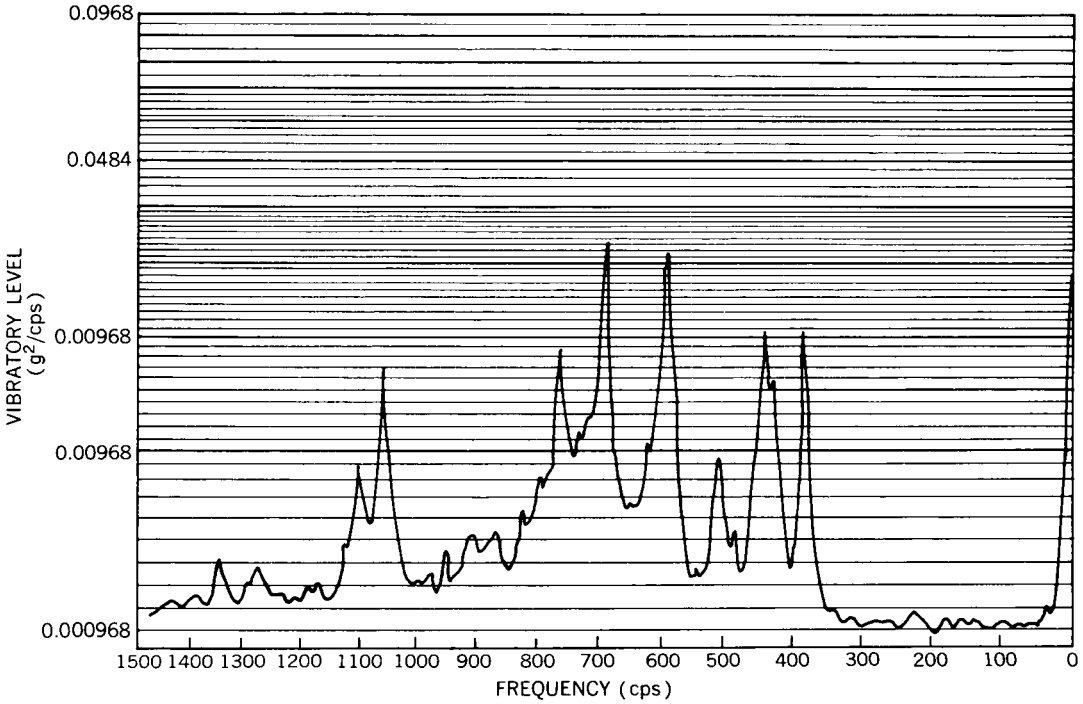

(a) AVT-1, T+31 to T+33 seconds

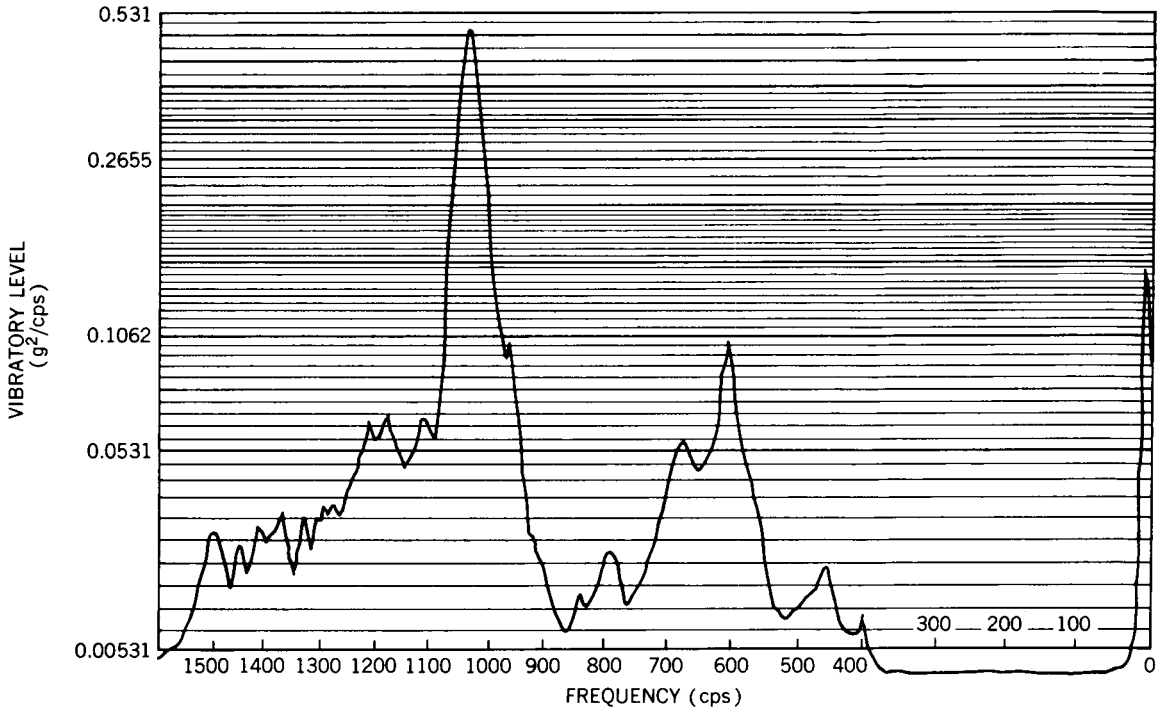

(b) AVT-2, T+38 to T+40 seconds

Figure 14—PSD plot, longitudinal axis. Filter bandwidth, 20 cps; RC averaging time, 1 sec; sample length, 2 sec.

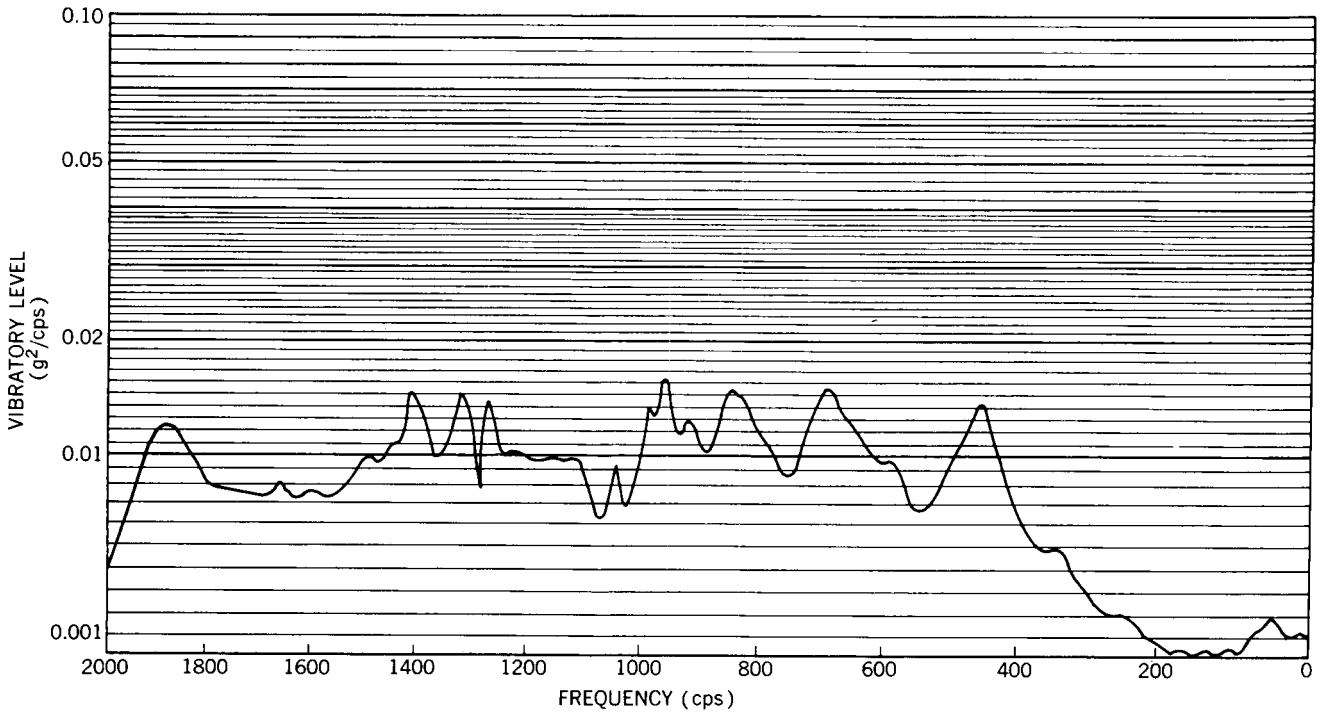

(a) AVT-1, T+37 to T+39 seconds

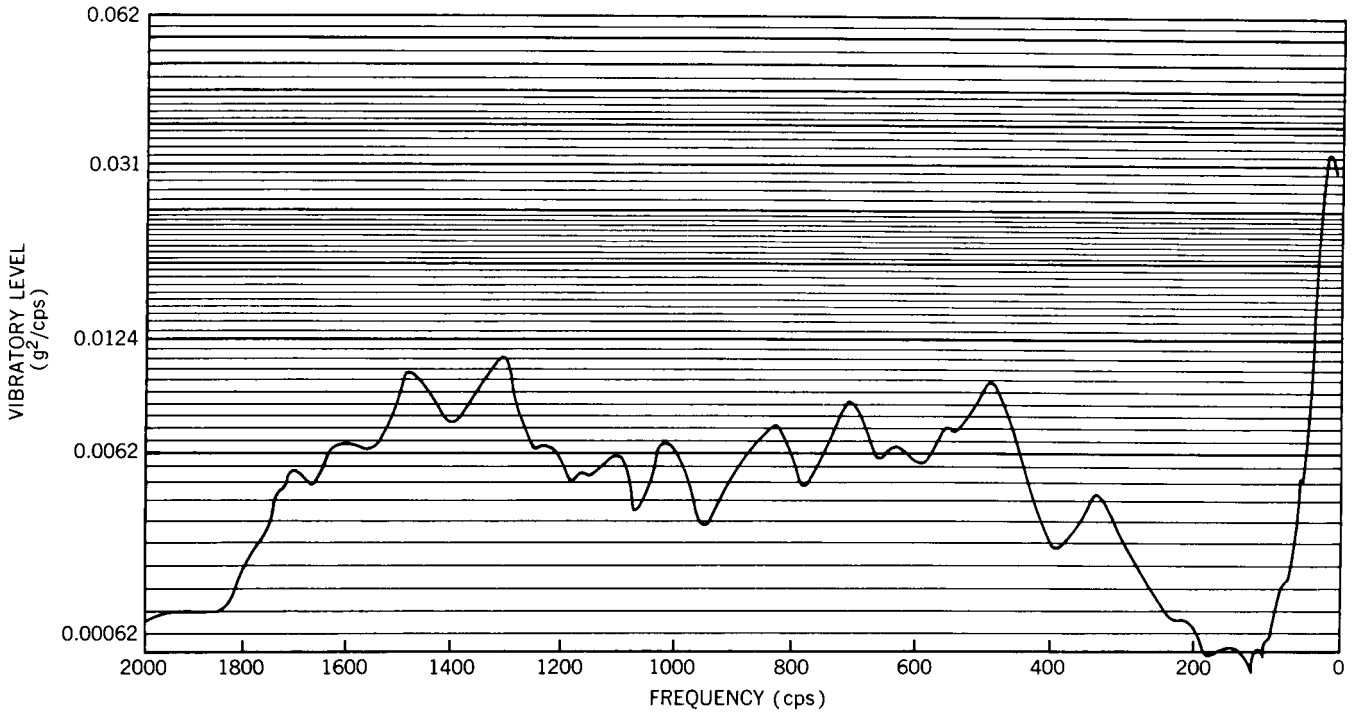

(b) AVT-2, T+38 to T+40 seconds

Figure 15—PSD plot, pitch axis. Filter bandwidth, 50 cps; RC averaging time, 1 sec; sample length, 2 sec.

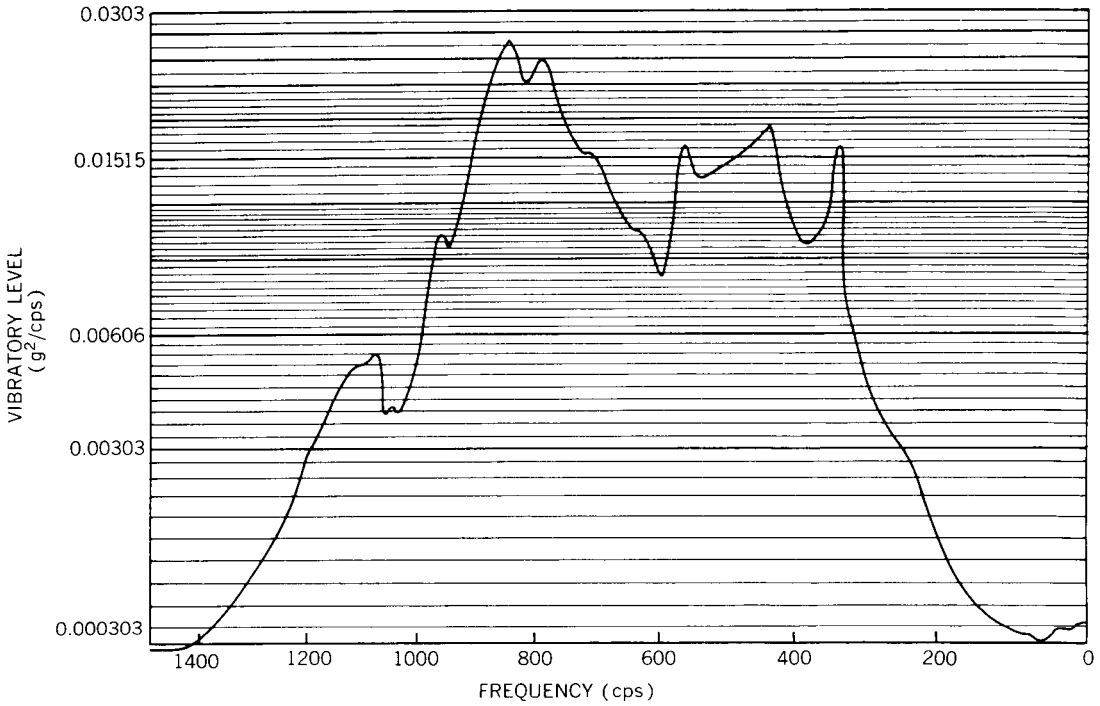

(a) AVT-1, T+37 to T+39 seconds

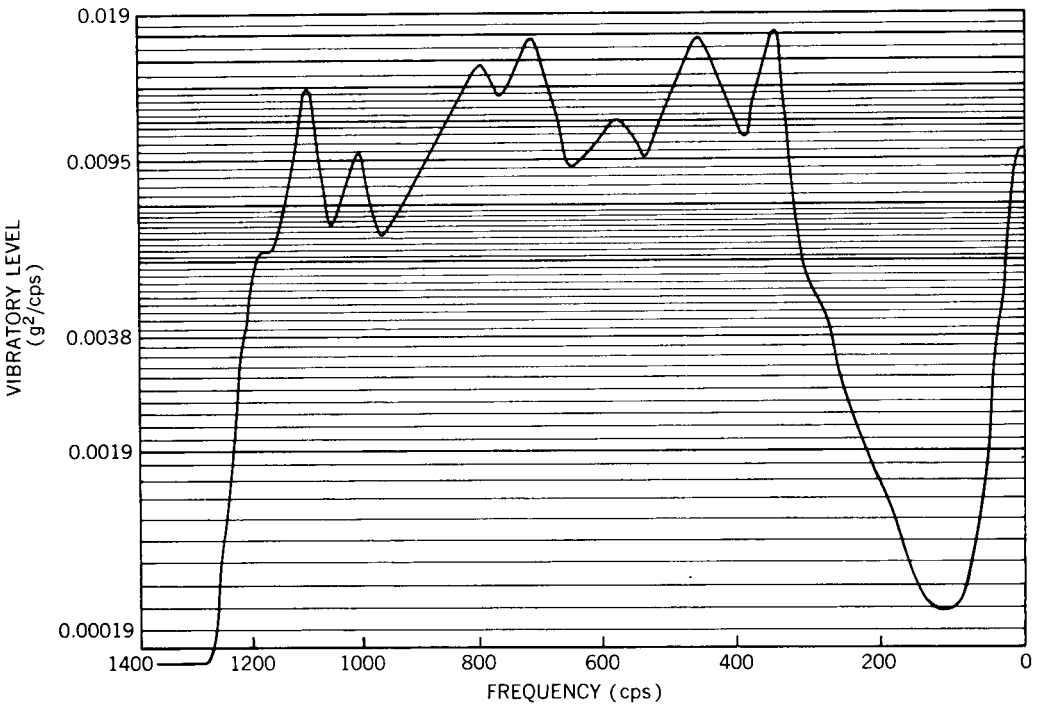

(b) AVT-2, T+38 to T+40 seconds

Figure 16—PSD plot, yaw axis. Filter bandwidth, 50 cps; RC averaging time, 1 sec; sample length, 2 sec.

along with the frequencies obtained during liftoff of AVT-2, and indicates the similarity of the frequencies measured. It is significant to point out the high PSD level (0.488 g^2/cps) measured at 1030 cps along the longitudinal axis of AVT-2 at T+39 seconds. The equivalent g-rms level in the region 940 cps to 1120 cps (see Figure 14b) is 6.62 g-rms, whereas the overall level at this time was 9.4 g-rms. PSD levels of AVT-1 given in Table 5 are not comparable to AVT-2 levels. AVT-1 data were not obtained at the same time, since the maximum level was clipped by the measuring system.

Figure 17 presents the probability density curves of the data loops used for the PSD analyses and compares them to a Gaussian distribution. Figure 18 gives a distribution curve obtained from data measured along the longitudinal axis of AVT-1 during time T+37 to T+39 seconds. The curve clearly illustrates "clipping" at -1.90σ and $+2.20\sigma$. Although the plots show that the probability distribution of the data are non-Gaussian, the deviation is slight.

Table 5

Comparison of Predominant Frequencies Measured Along the Longitudinal Axis of AVT-1 and AVT-2.*

AVT-1 (T+31 to T+33) PSD Analysis		AVT-2 (T+38 to T+40) PSD Analysis		AVT-2 (T+1 to T+2) Spectral Analysis	
Freq. (cps)	Level (g^2/cps)	Freq. (cps)	Level (g^2/cps)	Freq. (cps)	Relative Level
–	–	–	–	130	0.09
380	0.0198	–	–	330	.09
420	.0202	–	–	430	.32
480	.0046	470	0.02	–	–
510	.0091	–	–	–	–
580	.035	600	.102	580	.49
620	.0078	–	–	640	.60
680	.0321	660	.058	680	.51
700	.0096	–	–	720	.38
750	.0181	–	–	–	–
810	.006	790	.024	780	.41
860	.005	840	.014	830	.35
–	–	900	.028	–	–
–	–	950	.102	960	.43
1020	.0163	1020	.488	1030	.51
1100	.0085	1120	.066	–	–
–	–	1180	.069	1160	.31
–	–	1220	.065	–	–
1280	.0038	1280	.035	1260	.25
1340	.0039	1320	.032	1340	.16
–	–	1380	.033	–	–
–	–	1440	.026	–	–
–	–	1500	.029	1490	.27
				1700	.05
				1780	.10

*Filter bandwidth, 20 cps.

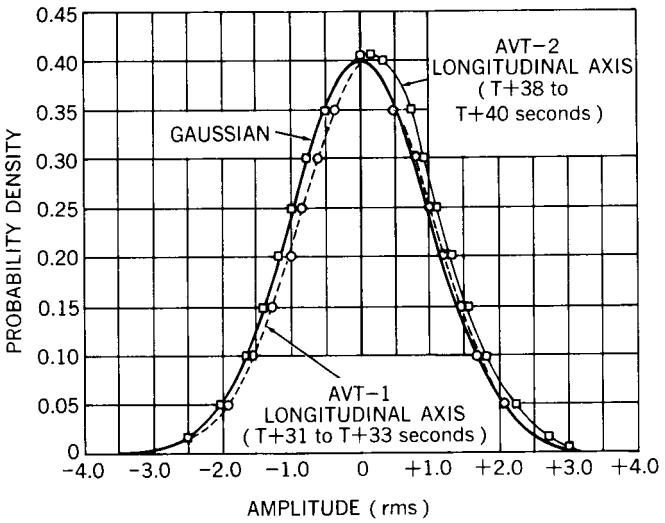

(a) Longitudinal axis

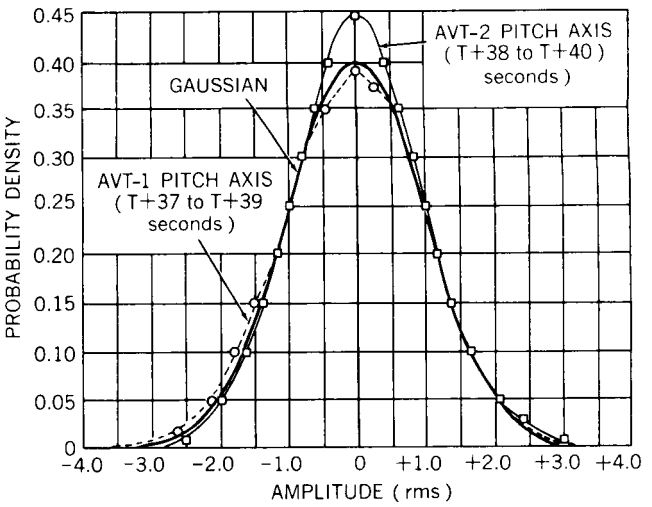

(b) Pitch axis

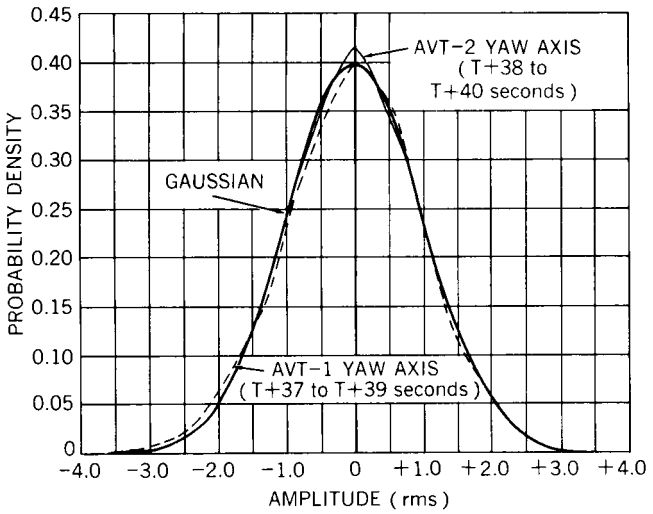

(c) Yaw axis

Figure 17—AVT-1 and AVT-2 probability density curves. Gaussian distribution, $Y = \frac{1}{\sqrt{2\pi}} e^{-x^2/2}$.

Comparison of AVT Data

The vibration data obtained from Echo A-12 application vertical tests include data measured during the flights of AVT-1 and AVT-2 and data measured during a vibration survey performed on the AVT-2 equipment compartment. The vibration survey was performed on the fully assembled AVT-2 vehicle on its launch pad at Cape Canaveral. Low-level sinusoidal vibration inputs (15 to 2000 cps) into the equipment compartment were accomplished by attaching two 25-pound electromagnetic shakers to the nose fairing dummy explosive bolts located 180 degrees apart at station 52.05. Response to sinusoidal excitations was measured by the flight transducers and by transducers mounted at various external locations on the equipment compartment. Figure 19 shows a physical arrangement of the test setup. In addition to the sinusoidal test, the equipment compartment natural frequencies were excited by striking the vehicle at various locations and directions at station 52.05 with a rubber mallet. A comparison of the AVT-2 flight data, vibration survey data, and the AVT payload vibration flight-acceptance-test specification levels is given in Table 6. The comparison indicates that resonant frequencies excited manually by mallet and those excited by the electromagnetic shakers were the predominant frequencies determined from the PSD analyses of the flight vibration data. It may be remembered that similar predominant frequencies occurred during liftoff, MECO, fairing separation, and spacecraft separation (Table 3).

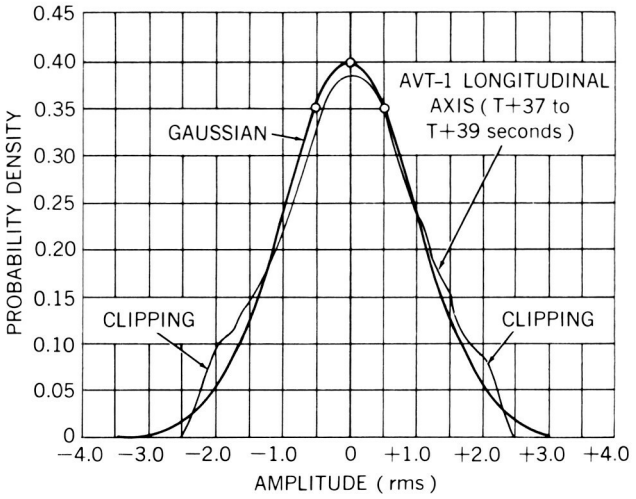

Figure 18–AVT-1 probability density curve, longitudinal axis. Gaussian distribution, $Y = \frac{1}{\sqrt{2\pi}} e^{-x^2/2}$.

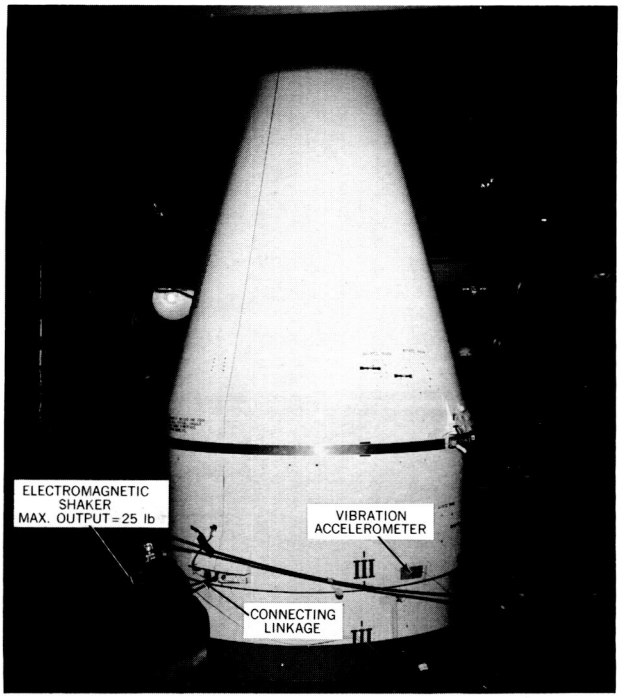

Figure 19–AVT-2 ground vibration survey test setup.

One of the effects of buffeting is the acoustical excitation of random vibrations in the vehicle and payload structures. Buffeting is usually defined as the result of unstable flow over the body and generally occurs as the vehicle approaches transonic speeds. The flow instability is independent of body motion but is directly related to the vehicle nose shape. References 1, 2, and 3 report recent studies of buffeting forces on certain types of vehicle nose shapes. Figure 20 shows the nose shapes of three vehicles used to launch the S-51 (Thor-Delta), Transit BI (Thor-Able-Star), and AVT (Thor); from this comparison, it might be

Table 6

Comparison of Flight Vibration Data with Ground Vibration Survey Frequencies and Test Specification Levels*

Ground Vibration Data, Thrust			AVT-2 Flight Vibration Data, Power Spectral Density*				Flight Test Levels, Sinusoidal	
Tapping	Forced Vibration							
Freq. (cps)	Freq. (cps)	Response (± g)	Freq. (cps)	Yaw (g^2/cps†)	Pitch (g^2/cps‡)	Thrust (g^2/cps**)	Freq. Range (cps)	Level
210	–	–	–	–	–	–	5-14	$\frac{1}{4}$ inch D. A.
400	390	3.3	340	0.0171	0.0071	–	14-400	4 g-rms
435	490	5.8	470	.0169	.0098	0.02		
–	585	4.6	575-625	.0114	.0065	.102	400-2000	6 g-rms
–	–	–	675-710	.0168	.0088	.058		
–	795	5.3	775-825	.0148	.0076	.024		
915	915	8.3	900	–	–	.028		
–	970	8.8	950	–	–	.102		
–	1040	10	1030	.0098	.0066	.488		
1100	1120	7.4	1100	.0133	.0062	.066		
1180	–	–	1180	–	–	.069		
1250	1200	6.4	1220	.0060	.0063	.065		
–	–	–	1280	–	–	.035		
–	–	–	1320	–	.0012	.032		
–	–	–	1380	–	–	.033		
–	–	–	1440	–	–	.026		
1570	1550	5.7	1500	–	.014	.029		
–	–	–	1630	–	.0067	–		
							Gaussian Random	
							15-2000 cps	0.045 g^2/cps (9.5 g-rms)

*Data sample measured at maximum flight vibration level, T+38 to T+40 seconds.
†Filter bandwidth, 50 cps.
‡Filter bandwidth, 50 cps.
**Filter bandwidth, 20 cps.

expected that the highest vibratory levels due to buffeting would be measured on the Thor-Able-Star vehicle and the lowest on the Thor-Delta vehicle. Figure 21, which compares the overall rms flight vibratory levels for these three vehicles,* confirms that the vibratory levels at transonic speeds were highest on the Thor-Able-Star and lowest on the Thor-Delta.

*Thor-Able-Star data were obtained from Reference 4, and Thor-Delta data from unpublished results by L. A. Williams of GSFC.

A comparison of the flight-measured values with the flight test specification (Table 6) indicates that the previously written test specification is both adequate and not overly severe. The flight-measured overall level of 9.4 g-rms, at transonic speeds, is slightly below the test specification of 9.5 g-rms random excitation. However, since the predominant excitation occurred in the frequency band of 940 to 1120 cps with an overall excitation level of 6.62 g-rms over this bandwidth (corresponds to a PSD of 0.488 g^2/cps), it is felt that the sinusoidal sweep at the level of 6 g-rms adequately simulates the flight vibration environment.

CONCLUDING REMARKS

The flight data presented in this report indicate that (1) the major vibration levels measured during the AVT flights occurred

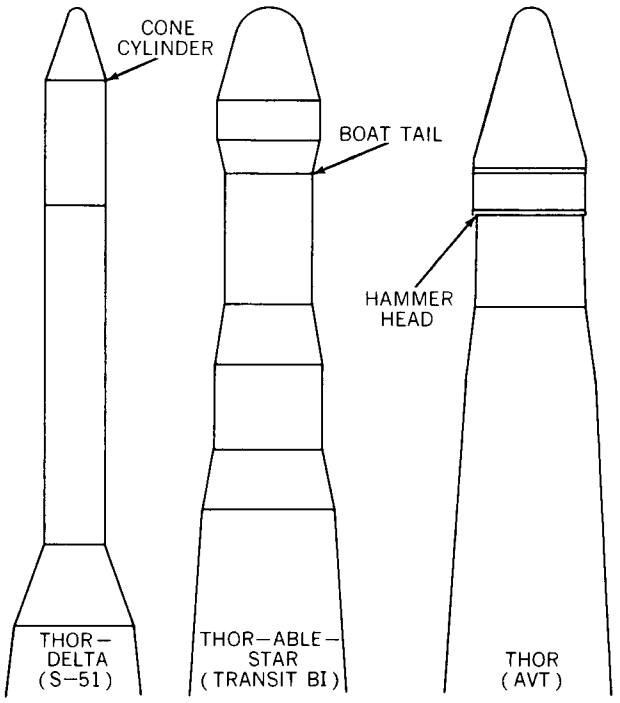

Figure 20—Comparison of AVT, Thor-Delta, and Thor-Able-Star nose shapes.

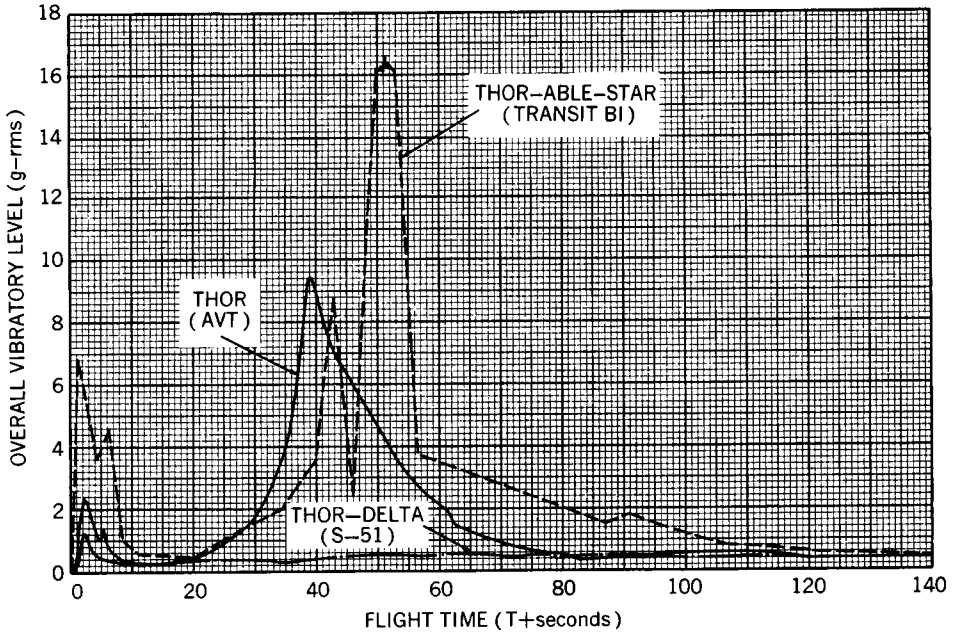

Figure 21—Longitudinal vibration–time history comparison of AVT, Thor-Delta, and Thor-Able-Star flights.

during liftoff, Mach 1, fairing separation, and payload separation; (2) the composite levels of both flights measured during these occurrences are in close agreement; (3) the spectra (level and frequency) are similar for comparative time data samples; and (4) the frequencies measured during flight were similar to those measured during the ground vibration survey.

Payload vibration data measured during a recent Thor-Delta flight show that no increase in level was measured during Mach 1 or maximum dynamic pressure; in contrast, high vibration levels were measured on the AVT flights. Also, high vibration levels were measured at Mach 1 and maximum dynamic pressure during flights of the Thor-Able-Star. The differences in the vibratory levels of these vehicles measured at transonic speeds are attributed mainly to the vehicle nose shape.

A comparison of the flight-measured vibration levels with the environmental flight acceptance test specification indicates that the previously written test specification is both adequate and not overly severe.

REFERENCES

1. Woods, P. and Ericsson, L. E., "Aeroelastic Considerations in a Slender, Blunt-Nose, Multistage Rocket," *Aerospace Eng.* 21(5):42-51, May 1962.
2. Coe, C. F., "Steady and Fluctuating Pressures at Transonic Speeds on Two Space-Vehicle Payload Shapes," NASA TM X-503, March 1961.
3. Coe, C. F., "The Effects of Some Variations in Launch-Vehicle Nose Shape on Steady and Fluctuating Pressures at Transonic Speeds," NASA TM X-646, March 1962.
4. Douglas, D. G., "Measurement and Analysis of Missile Vibration, Shock, and Noise Environments," *Proc. Instrum. Soc. Amer.* 17(2): Paper No. 38.1.62, 1962.